The functional reach of the hippocampal memory system to the oculomotor system

Abbreviated title: Hippocampal Responses Reach Oculomotor Regions

Jennifer D. Ryan[1,2*], Kelly Shen[1*], Arber Kacollja[1], Heather Tian[1], John Griffiths[1], Gleb Bezgin[3], Anthony R. McIntosh[1,2]

[1]Rotman Research Institute, Baycrest, Toronto, Ontario, M6A2E1
[2]Department of Psychology, University of Toronto, Toronto, Ontario M5S 3G3
[3]Montreal Neurological Institute, McGill University, Montreal, Quebec, QC H3A 2B4
** equal contribution*

Corresponding Authors:
Jennifer D. Ryan, PhD
Rotman Research Institute
Baycrest
3560 Bathurst St.
Toronto, ON M6A2E1
Email: jryan@research.baycrest.org

Kelly Shen, PhD
Rotman Research Institute
Baycrest
3560 Bathurst St.
Toronto, ON M6A2E1
Email: kshen@research.baycrest.org

Number of Pages: 42
Number of Figures: 3
Number of Tables: 9
Multimedia: N/A
Number of Words Abstract: 246
Number of Words Introduction: 634
Number of Words Discussion: 1497

Conflicts of Interest: The authors declare no competing financial interests.
Acknowledgments: The authors wish to thank R. Shayna Rosenbaum for her helpful comments on a previous version of this manuscript. This work was funded by a grant from Natural Sciences and Engineering Research Council of Canada to J.D.R.

Abstract

Visual exploration is related to activity in the hippocampus (HC) and/or extended medial temporal lobe system (MTL), is influenced by stored memories, and is altered in amnesic cases. An extensive set of polysynaptic connections exist between the HC and oculomotor system; however, it is not known if HC responses ultimately influence neural activity in the oculomotor system, and the timing by which such neural modulation could occur. We conducted simulations of the functional interactions between the two systems in the macaque brain by leveraging The Virtual Brain, a software platform for connectome-based modelling. Stimulation of CA1, pre-subiculum, and MTL cortices each resulted in observable responses in oculomotor regions, including the frontal eye fields (FEF), within the time of a fixation (<200ms). Stimulation of the subiculum and para-subiculum resulted in slower responses to FEF (400+ms), and CA3 stimulation did not reach FEF. Activity indicative of feedback from oculomotor regions was observed in cortical regions (areas 5, 7a, posterior cingulate) known for representing spatial frames of reference. Modeled lesions to the entorhinal, parahippocampal, and perirhinal cortices each slowed the dissipation of HC signal to oculomotor regions, whereas HC lesions generally did not affect the rapid MTL activity propagation (<100ms) to oculomotor regions. These findings provide novel evidence that information represented by the HC/MTL activity may influence the oculomotor system during the time of a gaze fixation. HC lesions may result in an increased rate of visual exploration due to the remaining, and relatively faster, signal from MTL regions.

Significance Statement

No major account of oculomotor (eye movement) guidance considers the influence of the hippocampus (HC) and broader medial temporal lobe (MTL) system, yet it is clear that information is exchanged between the two systems. Prior experience influences current viewing, and cases of amnesia due to compromised HC/MTL function show specific alterations in viewing behaviour. Using computational modeling, we show that stimulation of subregions of the HC, and of the MTL, rapidly results in observable responses in oculomotor control regions, and that HC/MTL lesions alter signal propagation. These findings suggest that information from memory may readily guide visual exploration, and calls for a reconsideration of the neural circuitry involved in oculomotor guidance.

Introduction

Memory influences ongoing active exploration of the visual environment (see Hannula et al., 2010, for review). For instance, more viewing is directed to novel versus previously viewed items (Fantz, 1964; Fagan, 1970), and more viewing is directed to areas that have been altered from a prior viewing (Ryan et al., 2000; Smith, Hopkins, & Squire, 2006). Amnesic cases who have severe memory impairments due to compromised function of the hippocampus (HC) and/or broader medial temporal lobe (MTL) show changes in their viewing behavior compared to neurologically-intact cases (Ryan et al., 2000; Hannula et al., 2007; Warren et al., 2010; Chau et al., 2011; Olsen et al., 2015). Similar findings have been observed in older adults who have suspected HC/MTL compromise (Ryan et al., 2007), and certain viewing patterns have been shown to track with entorhinal cortex (ERC) volumes (Yeung et al., 2017). Visual exploration predicts HC activity during encoding (Liu et al., 2018), and, conversely, HC/MTL activity predicts ongoing visual exploration that is indicative of memory retrieval (Hannula & Ranganath, 2009; Ryals et al., 2015). The relationship between visual sampling and HC activity is weakened in aging, presumably due to decline in HC structure or function (Liu et al., 2018). Such evidence collectively demonstrates that HC/MTL function is related to oculomotor *behavior.* The indirect implication of these studies is that the HC must influence *neural activity* in the oculomotor system.

Studies in non-human primates have shown that HC/MTL activity is linked to oculomotor behavior. The activity of grid cells in the ERC are tied to eye position (Killian, Jutras, & Buffalo, 2012), while HC/MTL activity is modulated by saccades (Sobotka, Nowicka, & Ringo, 1997) and fixations (Hoffman et al., 2013; 2013; Leonard

et al., 2015). How HC/MTL activity traverses the brain to influence the oculomotor system has not been shown to date. There are no known direct connections in the non-human primate between hippocampal subfields and the oculomotor system. Yet, we have shown that there is an extensive set of polysynaptic pathways spanning extrastriate, posterior parietal, and prefrontal regions that may mediate the exchange of information between the oculomotor and memory systems (Shen, Bezgin, Selvam, McIntosh & Ryan, 2016). Prior work has speculated as to which regions of the brain may be important for transmitting information between the HC and oculomotor systems (e.g., Meister and Buffalo, 2017; Micic et al., 2010), but such discussions were limited to regions examined in isolation without considering the large and complex contribution of recurrent connections to the functional dynamics of large-scale brain networks. This limits our ability to examine a crucial question: is HC/MTL activity able to influence activity in the oculomotor system? In order to impact ongoing visual exploration, HC/MTL activity would likely need to resolve in the oculomotor system within the time of an average duration of a gaze fixation (~ 250-400 ms; Henderson, Nuthmann, Luke, 2013).

To examine the extent to which HC/MTL activity could influence activity in the oculomotor system, we leveraged a computational modeling and neuroinformatics platform, The Virtual Brain (TVB; thevirtualbrain.org) in combination with a macaque large-scale network. HC subregions and MTL cortices were each stimulated separately within the connectome-based model and the dissipation of activity through pre-identified cortical anatomical pathways (Shen et al., 2016) was observed (Spiegler et al 2016). Critically, we examined whether activity culminated in responses in key regions within the oculomotor system that provide motoric (e.g., frontal eye fields, FEF) and cognitive

control (e.g., dorsolateral prefrontal cortex, dlPFC; anterior cingulate, ACC) of eye movements (Johnston & Everling 2008). Finally, we observed the extent to which the propagation and timing of such activity was altered following lesions to one or more HC/MTL regions in order to understand the underlying neural dynamics that may result in altered visual exploration in cases of HC/MTL dysfunction, such as in amnesia or aging.

Methods

Large-scale network dynamics were simulated using TheVirutalBrain software platform. The connectome-based model represented each node of the network as a neural mass, all coupled together according to a structural connectivity matrix which constrains the spatial and temporal interactions of the system (Deco et al 2011; Breakspear 2017).

Data

A macaque network with 77 nodes of a single hemisphere was defined using the FV91 parcellation (Felleman & Van Essen 1991) and its structural connectivity was queried using the CoCoMac database of tract tracing studies (cocomac.g-node.org; Stephan et al 2001 Phil Trans Roy Soc B Bakker et al 2012 Frontiers in Neuroinformatics). A review of the extant literature was also performed to ensure the accuracy of anatomical pathways within and across MTL and oculomotor systems (see Shen et al 2016). Self-connections were not included in the connectivity matrix.

As CoCoMac only provides categorical weights for connections (i.e., weak, moderate or strong), we ran probabilistic tractography on diffusion-weighted MR imaging data from 10 male adult macaque monkeys (9 *Macaca mulatta*, 1 *Macaca*

fascicularis, age 5.8 ± 1.9 years) using the FV91 parcellation to estimate the fibre tract capacities and tract lengths between regions. Image acquisition, preprocessing and tractography procedures for this particular dataset have been previously described (Shen et al 2019; Shen et al 2018). Fiber tract capacity estimates (i.e., 'weights') between each ROI pair were computed as the number of streamlines detected between them, normalized by the total number of streamlines that were seeded. Connectivity weight estimates were averaged across animals and applied to the tracer network, keeping only the connections that appear in the tracer network. The resulting structural connectome was therefore directed, as defined by the tracer data, and fully weighted, as estimated from tractography. Tract lengths were also estimated using probabilistic tractography.

Node dynamics

The dynamics of each node in the macaque network were given by the following generic 2-dimensional planar oscillator equations:

$$\begin{aligned} \dot{V}_i &= \tau(-fV_i^3 + eV_i^2 + gV_i + \alpha W_i + \xi \sum_{j=1}^{N} w_{ij} V_j(t - \Delta_{ij}) + \gamma I \\ \dot{W}_i &= \tau^{-1}(cV_i^2 + bV_i - \beta W_i + a) \end{aligned}$$

where the fast variable V represents mean subthreshold neural activity (i.e., local field potential) at node i, W is a slower timescale recovery variable; the differential time constants of V vs. W are controlled by the time scale separation parameter τ.

The local coupling is scaled by g, while the global connectivity scaling factor ξ acts on all incoming connections to each node, which are also weighted individually by the connectivity weights matrix w (as described above). Exogenous stimulation currents

of interest in the present study enter the system through the input variable I. Transmission between network nodes was constrained according to the conduction delays matrix $\Delta = L/v$, where L is a matrix of inter-regional tract lengths and v is axonal conduction velocity. As in Spiegler et al. (2016), cubic, quadratic, and linear coefficients for V and W were set such that the dynamics reduce to a classic Fitzhugh-Nagumo system. Additional model parameters are listed in Table 1.

Brain dynamics operate near criticality when at rest (Ghosh et al., 2008). In this state, the nodes will naturally oscillate with constant magnitude. Setting the local parameter g so that the system operates near criticality will allow the node respond with a strong amplitude, and a longer lasting oscillation. If far from the critical point, the amplitude responses will be weak, slow, and fade quickly, and if spreading within a network, the excitation will decay quickly as it travels. Given our network's structure, re-entry points allow a node to be re-stimulated, making the excitation last longer and travel farther through the network (Spiegler et al., 2016). Following Spiegler et al. (2016), we tuned the model parameters such that the working point of each node was in a critical regime. The system of delay-differential equations shown above were solved numerically using a Heun Deterministic integration scheme, with step size dt=0.1 ms.

Model tuning & stimulation parameters

Simulations were run for 7000 ms, with stimulus onset occurring after 5000 ms to allow for settling of the initial transient resulting from randomly specified initial conditions. A single pulsed stimulus was used, with duration of 100 ms. To determine when nodes became active following stimulation, we first computed the envelope of each node's timeseries using a Hilbert transform. Each node's baseline activity was taken as the mean

amplitude of the envelope in the 200 ms prior to stimulation. The activation threshold of each node was defined as the baseline activity ± 2 std and activation time of each node was taken as the time its envelope amplitude surpassed the activation threshold.

To create a biologically realistic model, we stimulated V1 to find activation times of the following areas: V1, V2, V3, V4, middle temporal and medial superior temporal. Conduction velocity (v) was set to 3.0 m/s, and was within the range of conduction velocities estimated in empirical studies of the macaque brain (Girard, Hupé, Bullier, 2001; Caminiti et al., 2013). Activation times following V1 stimulation were compared to available empirical data (Schmolensky et al., 1998) and relevant model parameters were adjusted accordingly. Global coupling ξ was set to 0.012. The parameter g was set to -0.1 such that the system operated close to the criticality by dampening local excitability. Stimulus weighting (γ) was set to 0.03. Using these model parameters, simulated response times of visual areas following V1 stimulation exhibited a pattern of activations resembling the known hierarchical processing organization of the visual system (V2: 4 ms, V3: 4 ms, V4: 8 ms, MT: 9 ms, MSTl: 37 ms, MSTd: 47 ms, FEF: 99 ms). Differences with empirical activation times (e.g., MST and FEF) may be due 1) a lack of subcortical-cortical pathways in our model; and 2) the use of the same conduction velocity for all connections.

The same model and stimulation parameters were then used to stimulate the subregions of the hippocampus (CA3, CA1, subiculum, pre-subiculum, para-subiculum), enthorinal cortex (ERC), areas 35 and 36 of the perirhinal cortex (PRC), and areas TF and TH of the parahippocampal cortex (PHC), to look for the activations of nodes whose

201 pathways may serve to mediate the exchange of information between the memory and
202 oculomotor systems (Shen et al., 2016). These nodes of interest included areas V2, V4,
203 7a, granular insular cortex, anterior cingulate cortex, 46, 12, proisocortex, 5, 10, 11,
204 orbitofrontal area 13, orbitofrontal area 14, 23, 25, 32,and 11. We further examined
205 whether activation was observed in regions important for oculomotor guidance, including
206 the dorsolateral prefrontal cortex (area 46), anterior cingulate cortex (area 24), and the
207 frontal eye fields.

208 Lesion models

209 Lesions of particular HC and MTL subregions were simulated by removing their afferent
210 and efferent connections to the rest of the network. Stimulations of other HC and MTL
211 sites were repeated on these lesion models.

212 Code availability

213 Simulations were carried out using the command-line (Python) version of
214 TheVirtualBrain (TVB) software package which is available for download at
215 http://thevirtualbrain.org. The customized TVB code for simulations is available upon
216 request.
217

Results

HC Subregion Stimulation

Stimulation of HC subregions CA1, S, PrS, and PaS resulted in observable responses in all of the cortical nodes of interest, and within regions 46, 24, and FEF, of the oculomotor system (for CA1 example, see Figure 1A). Within our oculomotor regions of interest, activity was first observed in area 46, followed by 24, and finally FEF, regardless of HC stimulation site. Stimulation of the PrS resulted in the fastest observable responses in these oculomotor areas (under 70 ms; Figure 2A). Stimulation of CA1 resulted in rapid activity that culminated in oculomotor regions in under 220 ms (Figure 2B). Stimulation of either the S or the PaS resolved into area 46 activity by 200 ms, into area 24 by 250 ms, and finally into FEF by 500 ms (Figure 2C-D). Responses were not observed in the majority of the pre-defined cortical hubs following CA3 stimulation, and activity did not culminate in observable responses in the oculomotor areas (Figure 1B). See Table 2 for activation times for all nodes of interest.

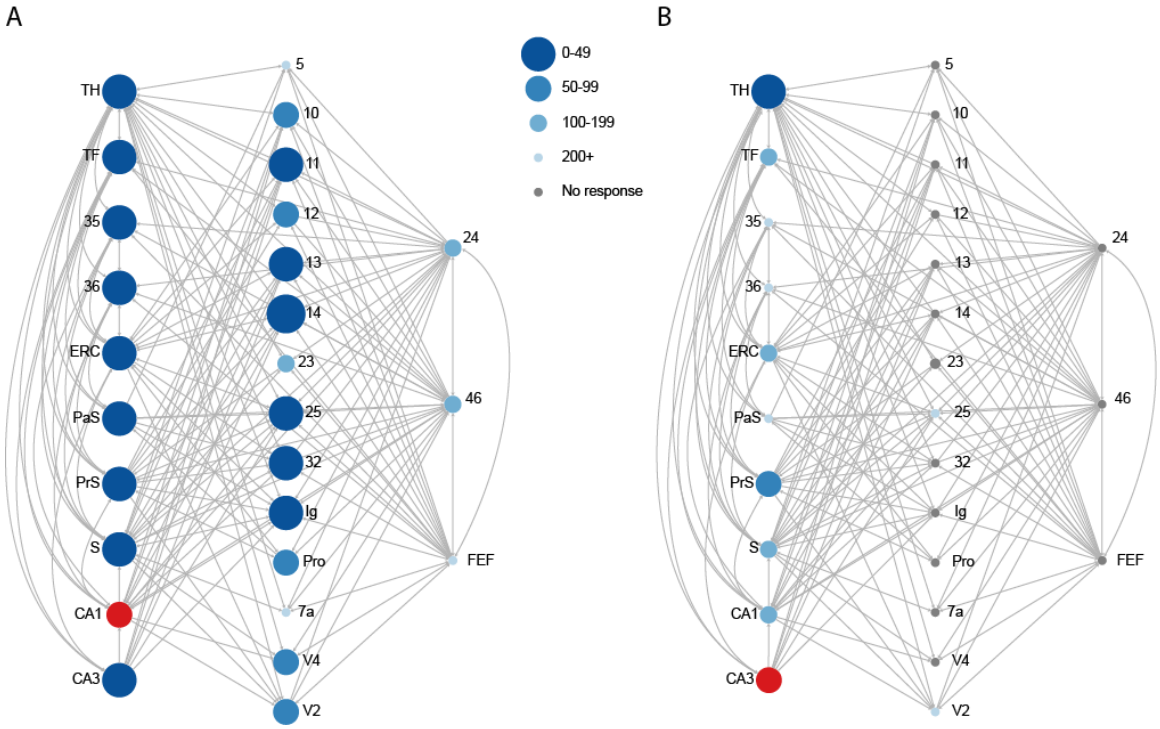

Figure 1. (A) Stimulation of the CA1 (red circle) resulted in observable responses (blue circles) in multiple HC/MTL nodes, intermediary nodes, and in regions governing oculomotor control, including the frontal eye fields (FEF). (B) Stimulation of the CA3 (red circle) resulted in observable responses (blue circles) limited to HC/MTL nodes. Very few responses were observed in oculomotor or cortical areas. Size and shade of the circles scale with elapsed time prior to an observed response. Grey lines denote direct structural connections between nodes. Only regions of interest - those that are involved in the shortest paths between HC/MTL and oculomotor nodes - are shown.

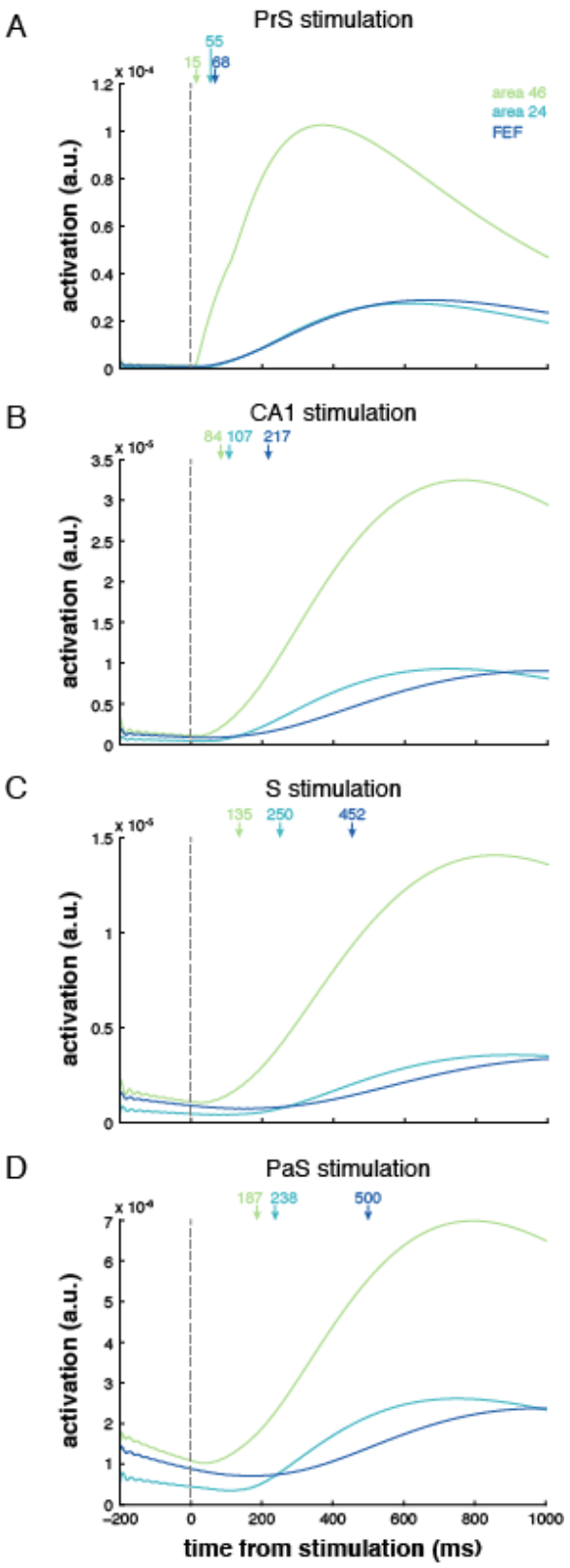

Figure 2. Response profiles (envelope of region time series) of oculomotor areas following stimulation of PrS (A), CA1 (B), S (C) and PaS (D). Activation is given in arbitrary units (a.u.). The onset of the response for areas 46, 24 and FEF indicated by green, blue and dark blue arrows, respectively.

MTL Stimulation

Stimulation of any of the broader regions within the MTL (ERC, 35, 36, TF, TH) resulted in observable responses within oculomotor areas 46, 24, and FEF well under 100ms, faster than the responses observed from HC subfield stimulation. Of the MTL regions, stimulation of area 35/36 resulted in the earliest responses in areas 46, 24, and FEF (within 25 ms). See Table 2 for activation times for all nodes of interest.

Cortical Responses

HC and MTL region stimulation (except for CA3) resulted in signal propagation across all of our pre-identified cortical regions of interest. When CA3 was stimulated, cortical responses were only observed in areas V2 and 25; no other signal was observed. Notably, responses in areas 5 and 7a were generally observed *following* activity from oculomotor regions, including FEF, suggestive of a possible feedback response. The exception is S stimulation, in which responses in area 5 preceded responses in oculomotor regions by ~100 ms. Responses in V4 also followed oculomotor responses; except in cases of CA1, TF, and TH stimulation. Likewise, responses in area 23 followed oculomotor responses, except in cases of PrS and TH stimulation. See Table 2 for activation times for all nodes of interest.

Lesion Models: HC subregions

Some models of HC and MTL lesions showed an appreciable effect on activation times while others did not. Only the results for lesions that affected any activation time by at least ±10 ms are shown. Lesion of CA3 changed neither the pattern nor the timing of observable responses following stimulation of each of the other HC/MTL regions (data not shown). Lesion of CA1 resulted in a lack of signal to V2, V4, and area 23, and

slowing of signal from the subicular complex to various regions, including the oculomotor regions (Figure 3A; Table 3). Lesion of CA1 also led to small increases in the speed of signal following CA3 stimulation to the subicular complex, and from MTL regions to TF/TH, and to other regions within the subicular complex (all less than 10 ms).

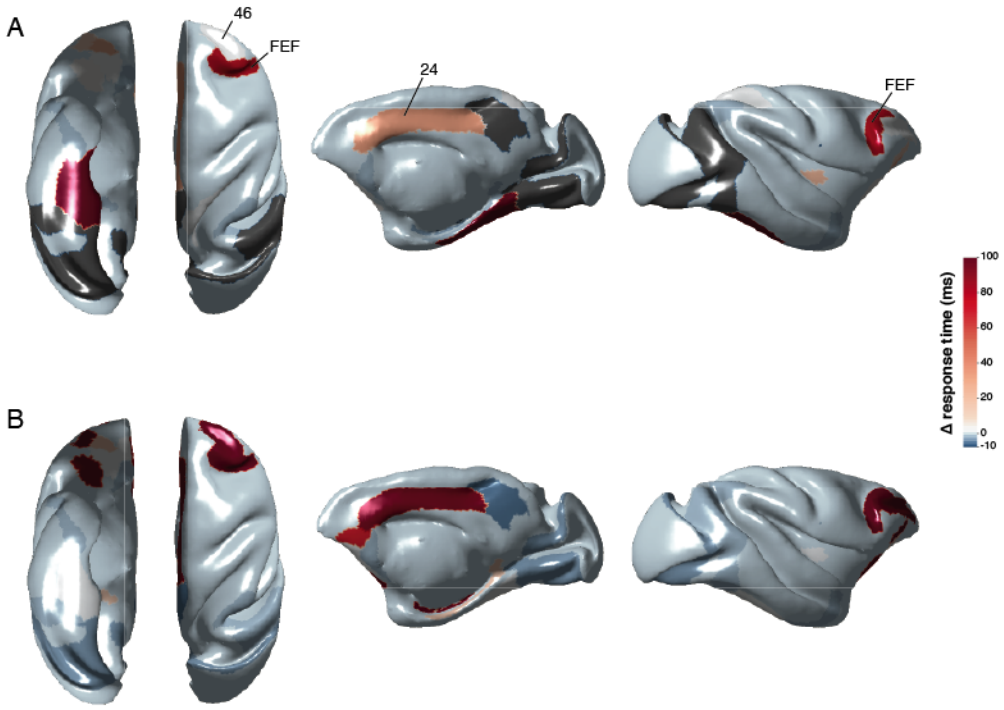

Figure 3. Changes in activation times following HC lesions. Subicular stimulation following CA1 (A) and ERC (B) lesions. Only nodes of interest are presented on the brain surface plots. Activation time differences were computed by subtracting the pre-lesion activation times from the post-lesion ones. Absence of response following a lesion indicated in grey.

Lesions to either the S or PaS produced little change to either the pattern or timing of responses following stimulation of the other HC/MTL regions (data not shown). Lesions to the PrS produced moderate changes (<20 ms) in timing: there was some slowing of activity propagation from PaS to some cortical regions, including oculomotor

287 regions, and some speeding of signal propagation within the HC subfields and to TF/TH
288 (Table 4).
289 A combined lesion to all HC subfields (CA3/CA1/S/PaS/PrS) did not
290 considerably change the pattern of signal propagation from the MTL cortices to
291 oculomotor regions. In cases where speeding/slowing was observed, the timing
292 differences were less than 15 ms, and mostly less than 10ms. Signal from the MTL
293 cortices still culminated within the oculomotor regions well under 50 ms (except for ERC
294 -> FEF at 79 ms) (Table 5).

295 Lesion Models: MTL regions

296 Lesion of the ERC resulted in considerable slowing of observable signal in oculomotor
297 regions (30-340ms) following S (Figure 3B) or PaS stimulation (Table 6). TF and/or TH
298 lesions resulted in slowing (10-400ms) of signal following CA1, S, and PaS stimulation
299 to one or more oculomotor regions, and a lack of response in FEF following PaS
300 stimulation (only the combined TF/TH is shown; Table 7). Area 35 and/or 36 lesions also
301 resulted in slowing (10-90ms) of signal following CA1, S, and PaS stimulation to one or
302 more oculomotor regions, although not as severe as the slowing observed following
303 TF/TH lesions (only the combined 35/36 lesion is shown; Table 8).

304 Other Cortical Lesions

305 In our original stimulations, signals in regions 5, 7a, 23, and V4 were predominantly
306 observed following observable responses in one or more of the oculomotor regions of
307 interest here, suggesting these cortical areas are receiving feedback signals rather than
308 primarily serving as hubs to transfer signal from the HC/MTL to the oculomotor regions.
309 To explore this in more depth, we did a combined lesion of 5/7a/23/V4 and examined

310 signal propagation. Following this combined cortical lesion, stimulation of each of the
311 HC/MTL regions (except for CA3) continued to result in observable signal in each of the
312 oculomotor regions (Table 9).
313

314 **Discussion**

315 A preponderance of evidence has demonstrated a relationship between HC/MTL neural
316 activity and oculomotor *behavior* (Liu et al., 2017; Leung et al., 2017, 2018; Killian,
317 Potter, Buffalo, 2015; Hannula et al., 2010), but research had not shown the influence of
318 the HC/MTL on oculomotor *activity,* and the HC/MTL are not considered in most models
319 of oculomotor control (e.g., Itti & Koch 2000; Hamker 2006; but see Belopolsky 2015).
320 The HC is well connected anatomically to the oculomotor system through a set of
321 polysynaptic pathways that span MTL, frontal, parietal, and visual cortices (Shen et al.,
322 2016), but, the existence of anatomical connections does not provide conclusive evidence
323 of functional relevance of specific pathways. Here, we show that propagation of
324 HC/MTL neural activity directly results in neural activity observable in area 24 (ACC)
325 and area 46 (dlPFC), and in the FEF, which are important for the cognitive and motoric
326 control of eye movements, respectively (Johnston & Everling, 2008). Critically, the
327 culmination of neural signal in one or more oculomotor control regions occurred within
328 the time of a typical gaze fixation (~250-400 ms; Henderson, Nuthmann, Luke, 2013;
329 Buswell, 1935): within 200 ms following HC subfield stimulation (except for CA3), and
330 within 100 ms following stimulation of each MTL region. Thus, the underlying neural
331 dynamics of the memory and oculomotor systems allow for representations mediated by

332 the HC/MTL to guide visual exploration – what is foveated and when – on a moment-to-
333 moment basis.

334 The lack of responses in the FEF following CA3 stimulation is not surprising,
335 given that there are no known direct connections, and fewer polysynaptic pathways,
336 between the CA3 and the oculomotor regions investigated here (Shen et al., 2016). The
337 functional and anatomical differences align well with the purported representational
338 functions of CA3 versus CA1. Foveated information may be bound into detailed memory
339 representations via the auto-associative network of the CA3 (*pattern separation;* Yassa &
340 Stark, 2011; Norman & O'Reilly, 2003), whereas CA1 would enable the comparison of
341 stored information to the external visual world (*pattern completion;* Yassa & Stark, 2011;
342 Rolls, 2013).

343 Stimulation of the subiculum and parasubiculum resulted in relatively slower
344 responses observed in each of the oculomotor regions, whereas stimulation of
345 presubiculum resulted in rapid responses observed in the oculomotor regions. The
346 subiculum and parasubiculum may largely provide information that supports the grid cell
347 mapping of the ERC (Tang et al., 2016; Peyrache, Schieferstein, Buzsaki, 2017; Boccara
348 et al., 2010). These regions may then function as a 'pointer' by providing online
349 information of an individual's location in space (Tang et al., 2016). This slowly changing
350 spatial layout may not then require a rapid influence on the oculomotor system, but
351 instead, may allow for the presubiculum, which has cells that are responsive to head
352 direction (Robertson et al., 1999) to precisely locate and foveate visual objects. These
353 functional distinctions are speculative, and remain to be tested.

Stimulation of each of the MTL cortices resulted in observable responses in each of the three oculomotor regions considered here that were faster than any of the responses observed following HC subregion stimulation. The MTL cortices are intermediary nodes that may permit the relatively rapid transfer of information from HC to the oculomotor system. The unique representational content supported by each region may influence ongoing visual exploration in a top-down manner. The PRC provides lasting information regarding the features of objects (Graham, Barense & Lee, 2010; Erez, Cusack, Kendall & Barense, 2016), the PHC provides information regarding the broader spatial environment (Alvarado & Bachevalier, 2005; Eichenbaum, Yonelinas, Ranganath, 2007; Sato & Nakamura, 2003), and the ERC may provide information regarding the relative spatial arrangements of features within (Yeung et al., 2017), and among objects within the environment (Buckmaster, Eichenbaum, Amaral, Suzuki & Rapp, 2004; Yeung et al., in press). Signal from the MTL may be used to accurately, and rapidly, prioritize gaze fixations to areas of interest.

HC subfield lesions only minimally altered the timing of activity from MTL to oculomotor regions; the relatively rapid propagation of signal from MTL to FEF (< 100ms) was preserved. Lesions to MTL regions resulted in slowing of signal from some HC subfields to oculomotor regions. This pattern of results suggests that different patterns of visual exploration (i.e., rate, area) may occur in cases of HC/MTL damage depending on the location of the lesion. Lesions restricted to HC subfields may result in an increase in the rate of gaze fixations due to the intact, rapid responses from the MTL to oculomotor regions. This is consistent with prior work in which a developmental amnesic case with HC subfield volume reductions showed an increase in gaze fixations

377 compared to control participants (Olsen et al., 2015). Similarly, older adults, who had
378 functional changes in the HC, showed increases in visual exploration (Liu et al., 2017).
379 ERC and PHC lesions may slow the use of information regarding the broader, ongoing
380 spatial environment; this could result in the need to continually revisit regions to re-
381 establish the relations within and among objects, and with their broader environment, and
382 thus an increased area of visual exploration and/or increase between-object gaze
383 transitions would be observed. Such behavior has been shown by older adults, which may
384 be related to structural and/or functional changes in the ERC (Chan, Kamino, Binns &
385 Ryan, 2012; Leung et al., 2017; 2019).

386 A future question for investigation is how distinct types of representations from
387 the HC/MTL are integrated and prioritized to influence visual exploration, including
388 saccade timing and the ordering of gaze fixations to distinct targets. Alternatively, the
389 functionally distinct representations of the HC/MTL may not actually be integrated
390 within the oculomotor system; rather, each may guide visual exploration at different
391 moments, as time unfolds, as new information in the visual world is sampled, and as task
392 demands are enacted and ultimately met. In either case, multiple memory 'signals' are
393 evident within patterns of gaze fixations, including memory for single stimuli (Althoff &
394 Cohen, 1999; Smith & Squire, 2017), memory for the relative spatial (and non-spatial)
395 relations within (Yeung et al., 2017), and among objects (Ryan et al., 2000; Smith,
396 Hopkins & Squire, 2006; Hannula et al., 2007). Dissociations in these memory signals
397 can be observed within single gaze patterns in neuropsychological cases (Ryan & Cohen,
398 2003).

399 Memory may influence visual exploration through multiple routes. Responses
400 emanating from the HC/MTL that ultimately resulted in observable responses in the
401 ACC, dlPFC, and FEF traversed through multiple frontal, visual, and parietal nodes.
402 Cortical responses were also observed *following* responses in the oculomotor regions.
403 Specifically, areas 5, 7a, 23 (posterior cingulate), and V4 may receive feedback from
404 oculomotor regions, rather than serving as hubs that relay information between the
405 HC/MTL and oculomotor systems (Meister & Buffalo, 2016). Area 5 has been implicated
406 in mapping visual and body-centered frames of reference to support visually-guided
407 reaching (Seelke et al., 2012). Cells in area 7a are responsive to eye position and saccades
408 (Bremmer, Distler, Hoffman, 1997). The posterior cingulate is part of the default mode
409 network (Buckner, Andrews-Hanna, Schacter, 2008; see Vincent, Kahn, Van Essen &
410 Buckner, 2010 for a homologous default mode network in primates) that is active during
411 internally directed cognitions. Neurons in V4 of the macaque are known to integrate
412 visual and oculomotor information, and show remapping of space towards that of a
413 saccade target, thereby bridging pre- and post-saccade spatial representations (Neupane,
414 Guitton, Pack, 2016). Information from the HC/MTL may guide gaze selection and
415 execution, and the resulting spatial selections are continually updated throughout cortex
416 to promote ongoing exploration, and feed back into memory.
417 It should be noted that future work remains to examine signal propagation across
418 subcortical-cortical pathways. The present work did not include such pathways because
419 although CoCoMac does contain tracer data regarding the presence/absence of thalamic
420 connections, it does not provide connection weights, which are critical to constraining the
421 dynamics of the model. We have validated the tractography methodologies used here for

422 estimating cortical connection strengths against available tracer data (Shen et al., 2019);
423 however, validated methods for running tractography in subcortical regions in macaques
424 do not currently exist. Nonetheless, a lack of subcortical considerations does not diminish
425 the evidence of the rapid communication between the hippocampal and oculomotor
426 systems via cortical routes, within the time window of a typical gaze fixation.
427 Neuropsychological, neuroimaging, and neurophysiological studies provide
428 important information regarding the representational content that is supported by distinct
429 regions of the brain. A network analysis approach can be instrumental in revealing the
430 broad dynamics by which such representational content governs behavior (Mišić, Goñi,
431 Betzel, Sporns, & McIntosh, 2014; Vlachos, Aertsen, & Kumar, 2012). Memory for
432 objects and their spatial relations provide rapid guidance for gaze prioritization and
433 accurate targeting for foveation. Disruptions to the HC/MTL result in an altered rate and
434 pattern of visual exploration (Olsen et al., 2015; Hannula, Ryan, Warren, 2017),
435 consistent with the dynamics of our lesion models. The present work calls for a
436 reconsideration of the neural architecture that supports oculomotor guidance: the
437 HC/MTL provides information to guide visual exploration across space and time.
438

References

Aggleton, J.P. (2012). Multiple anatomical systems embedded within the primate medial temporal lobe: Implications for hippocampal function. *Neuroscience and Biobehavioral Reviews, 36,* 1579-1596.

Althoff, R. R., and Cohen, N. J. (1999). Eye-movement based memory effect: a reprocessing effect in face perception. *Journal of Experimental Psychology: Learning, Memory, and Cognition, 25,* 997–1010.

Alvarado, M.C. & Bachevalier, J. (2005). Comparison of the effects of damage to the perirhinal and parahippocampal cortex on transverse patterning and location memory in rhesus macaques. *Journal of Neuroscience, 25(6),* 1599-1609.

Andersen, R.A., Essick, G.K., & Siegel, R.M. (1985). Encoding of spatial location by posterior parietal neurons. *Science, 230(4724),* 456-458.

Belopolsky A. (2015) Common priority map for selection history, reward and emotion in the oculomotor system. *Perception 44(8-9),* 920-933.

Boccara, C.N., Sargolini, F., Thoresen, V.H., Solstad, T., Witter, M.P., Moser, E.I., Moser, M.B. (2010). Grid cells in pre-and parasubiculum. *Nature Neuroscience, 13(8),* 987-994.

Bremmer, F., Distler, C., Hoffman, K.P. (1997). Eye position effects in monkey cortex. II. Pursuit- and fixation-related activity in posterior parietal areas LIP and 7A. *Journal of Neurophysiology, 77(2),* 962-977.

Buckmaster, C.A., Eichenbaum, H., Amaral, D.G., Suzuki, W.A., & Rapp, P.R. (2004). Entorhinal cortex lesions disrupt the relational organization of memory in monkeys. *Journal of Neuroscience, 24(44),* 9811-9825.

Buckner, R.L., Andrews-Hanna, J.R., Schacter, D.L. (2008). The brain's default network: anatomy, function, and relevance to disease. *Annals of the New York Academy of Sciences, 1124,* 1-38.

Buswell, G. T. (1935). *How people look at pictures*. Chicago, IL: University of Chicago Press.

Caballero-Bleda, M., Witter, M.P. (1993). Regional and laminar organization of projections from the presubiculum and parasubiculum to the entorhinal cortex: an anterograde tracing study in the rat. *Journal of Comparative Neurology, 328(1),* 115-129.

Caminiti, R., Carducci, F., Piervincenzi, C., Battaglia-Mayer, A., Confalone, G., Visco-Comandini, F., Pantano, P., Innocenti, G.M. (2013). Diameter, length, speed, and conduction delay of callosal axons in macaque monkeys and humans: comparing data from histology and magnetic resonance imaging diffusion tractography. *Journal of Neuroscience, 33(36),* 14501-11.

Chau, V.L., Murphy, E.F., Rosenbaum, R.S., Ryan, J.D. & Hoffman, K.L. (2011). A flicker change detection task reveals object-in-scene memory across species. *Frontiers in Behavioral Neuroscience, 5:58.*

Christiansen, K., Dillingham, C.M., Wright, N.F., Saunders, R.C., Vann, S.D., Aggleton, J.P. (2016). Complementary subicular pathways to the anterior thalamic nuclei and mammillary bodies in the rat and macaque monkey brain. *European Journal of Neuroscience, 43(8),* 1044–1061.

Dalton, M.A., & Maguire, E. A. (2017). The pre/parasubiculum: a hippocampal hub for scene-based cognition? *Current Opinion in Behavioral Sciences, 17,* 34-40.

Diana, R.A., Yonelinas, A.P., Ranganath, C. (2012). Adaptation to cognitive context and item information in the medial temporal lobes. *Neuropsychologia, 50(13),* 3062-3069.

Eichenbaum, H., Yonelinas, A.P., Ranganath, C. (2007). The medial temporal lobe and recognition memory. *Annual Review of Neuroscience, 30,* 123-152.

Erez, J., Cusack, R., Kendall, W., Barense, M.D. (2016). Conjunctive coding of complex object features. *Cerebral Cortex, 26(5),* 2271-2282.

Fagan, J. F. (1970). Memory in the infant. *J. Exp. Child. Psychol.* 9, 217–226.

Fantz, R. L. (1964). Visual experience in infants: Decreased attention to familiar patterns relative to novel ones. *Science* 146, 668–670.

Ghosh, A., Rho, Y., McIntosh, A., Kötter,R., Jirsa,V. (2008). Noise during rest enables the exploration of the brain's dynamic repertoire. *PLoS Computational Biology,* 4:e1000196. doi: 10.1371/journal.pcbi.1000196

Girard, P., Hupé, J.M., Bullier, J. (2001). Feedforward and feedback connections between areas of V1 and V2 of the monkey have similar rapid condition velocities. *Journal of Neurophysiology,* 85(3):1328-31.

Graham, K.S., Barense, M.D., & Lee, A.C. (2010). Going beyond LTM in the MTL: a synthesis of neuropsychological and neuroimaging findings on the role of the medial temporal lobe in memory and perception. *Neuropsychologia, 48(4),* 831-853.

Hamker F. (2006) Modeling feature-based attention as an active top-down inference process. *BioSystems, 86(1-3),* 91-99.

Hannula, D. E., Ryan, J.D., Tranel, D. & Cohen, N.J.. (2007). Rapid onset relational memory effects are evident in eye movement behavior, but not in hippocampal amnesia. *Journal of Cognitive Neuroscience, 19,* 1690-1705.

Hannula, D. E., and Ranganath, C. (2009). The eyes have it: hippocam pal activity predicts expression of memory in eye movements. *Neuron* 63, 592–599.

Hannula, D.E., Althoff, R.R., Warren, D.E., Riggs, L., Cohen, N.J. & Ryan, J.D. (2010). Worth a glance: using eye movements to investigate the cognitive neuroscience of memory. *Frontiers in Human Neuroscience, **4**:166. doi:10.3389/fnhum.2010.00166.*

Heisz, J.J. & Ryan, J.D. (2011). The effects of prior exposure on face processing in younger and older adults. *Frontiers in Aging Neuroscience, 3:15. doi: 10.3389/fnagi.2011.00015.*

Henderson, J.M., A. Nuthmann, S.G. Luke (2013). Eye movement control during scene viewing: Immediate effects of scene luminance on fixation durations. *Journal of Experimental Psychology: Human Perception and Performance*, *39(2),* 318–322.

Hoffman, K. L., Dragan, M. C., Leonard, T. K., Micheli, C., Montefusco-Siegmund, R., & Valiante, T. A. (2013). Saccades during visual exploration align hippocampal 3–8 Hz rhythms in human and non-human primates. *Frontiers in Systems Neuroscience, 7,* 43.

Itti L. & Koch, C. (2000) A saliency-based search mechanism for overt and covert shifts of visual attention. *Vision Research, 40(10-12),* 1489-1506.

Johnston, K., & Everling, S. (2008). Neurophysiology and neuroanatomy of reflexive and voluntary saccades in non-human primates. *Brain and Cognition, 68,* 271–283.

Killian, N. J., Jutras, M. J., & Buffalo, E. A. (2012). A map of visual space in the primate entorhinal cortex. *Nature, 491,* 761–764.

Killian, N.J., Potter, S.M., Buffalo, E.A. (2015). Saccade direction encoding in the primate entorhinal cortex during visual exploration. *Proceedings of the National Academy of Sciences USA, 112(51),* 15743-15748.

Lavenex, P., Lavenex, P.B. & Amaral, D.G. (2004). Nonphosphorylated high-molecular-weight neurofilament expression suggests early maturation of the monkey subiculum. *Hippocampus, 14(7),* 797-801.

Lavenex, P., Lavenex, P.B. (2013). Building hippocampal circuits to learn and remember: insights into the development of human memory. *Behavioral Brain Research, 254,* 8-21.

Leonard, T. K., Mikkila, J. M., Eskandar, E. N., Gerrard, J. L., Kaping, D., Patel, S. R., et al. (2015). Sharp wave ripples during visual exploration in the primate hippocampus. *Journal of Neuroscience, 35,* 14771–14782.

Liu, Z-X., Shen, K., Olsen, R.K. & Ryan, J.D. (2017). Visual sampling predicts hippocampal activity. *Journal of Neuroscience, 37(3),* 599-609.

Loftus, G. R., & Mackworth, N. H. (1978). Cognitive determinants of fixation location during picture viewing. Journal of Experimental Psychology. Human Perception and Performance, 4, 565–572.

Maass, A., Berron, D., Libby, L. A., Ranganath, C., and Duzel, E. (2015). Functional subregions of the human entorhinal cortex. *Elife* 4:e06426.

Meister, M.L.R., Buffalo, E.A. (2016). Getting directions from the hippocampus: The neural connection between looking and memory. *Neurobiology of Learning and Memory, 134,* 135-144.

Mišić, B., Goñi, J., Betzel, R.F., Sporns, O., & McIntosh, A.R. (2014). A network convergence zone in the hippocampus. *PLoS Computational Biology,*10(12):e1003982. doi: 10.1371/journal.pcbi.1003982.

Morris, R.G., Schenk, F., Tweedie, F., Jarrard, L.E. (1990). Ibotenate lesions of the hippocampus and/or subiculum: dissociating components of allocentric spatial learning. *European Journal of Neuroscience, 2(12),* 1016-1028.

Naber, P.A., Caballero-Bleda, M., Jorritsma-Byham, B., and Witter, M. P. (1997). Parallel input to the hippocampal memory system through peri- and postrhinal cortices. *Neuroreport, 8,* 2617–2621.

Neupane, S., Guitton, D., & Pack, C.C. (2016). Two distinct types of remapping in primate cortical area V4. *Nature Communications,* Feb 1;7:10402. doi: 10.1038/ncomms10402.

Norman, K.A., O'Reilly, R.C. (2003) Modeling hippocampal and neocortical contributions to recognition memory: a complementary-learning-systems approach. *Psychological Review, 110*, 611–646.

Olsen, R.K., Sebanayagam, V., Lee, Y., Moscovitch, M., Grady, C.L., Rosenbaum, R.S. & Ryan, J.D. (2016). The relationship between eye movements and subsequent recognition: Evidence from individual differences and amnesia. *Cortex, 85,* 182-193

Olsen, R.K., Lee, Y., Kube, J., Rosenbaum, R.S., Grady, C., Moscovitch, M. & Ryan, J.D. (2015). The role of relational binding in item memory: evidence from face recognition in a case of developmental amnesia. *Journal of Neuroscience, 35(13),* 5342-5350.

O'Mara, S. (2005). The subiculum: what it does, what it might do, and what neuroanatomy has yet to tell us. *Journal of Anatomy,* 207(3):271-82.

O'Mara, S.M., Commins, S., Anderson, M. & Gigg, J. (2001). The subiculum: a review of form, physiology, and function. *Progress in Neurobiology, 64(2),* 129-155.

Peyrache, A., Schieferstein, N. & Buzsaki, G. (2017). Transformation of the head-direction signal into a spatial code. *Nature Communication, 8(1),* 1752.

Robertson, R.G., Rolls, E.T., Georges-Francois, P., Panzeri, S. (1999). Head direction cells in the primate pre-subiculum. *Hippocampus, 9(3),* 206-219.

Rolls, E.T. & O'Mara, S.M. (1995). View-responsive neurons in the primate hippocampal complex. *Hippocampus, 5(5),* 409-424.

Rolls, E.T. (2013). The mechanisms for pattern completion and pattern separation in the hippocampus. *Frontiers in System Neuroscience,* 7: 74. doi: 10.3389/fnsys.2013.00074

Ryals AJ, Wang JX, Polnaszek KL, Voss JL (2015) Hippocampal contribution to implicit configuration memory expressed via eye movements during scene exploration. *Hippocampus, 25,* 1028 –1041.

Ryan, J.D., Hannula, D.E., & Cohen, N.J.. (2007). The obligatory effects of memory on eye movements. *Memory, 15(5),* 508-525.

Ryan, J.D., Leung, G.L., Turk-Browne, N.B., & Hasher, L. (2007). Assessment of age-related changes in inhibition and binding using eye movement monitoring. *Psychology and Aging, 22,* 239-250.

Ryan, J.D. & Cohen, N.J. (2003). Evaluating the neuropsychological dissociation evidence for multiple memory systems. *Cognitive, Affective and Behavioral Neuroscience, 3(3)*, 168-185.

Ryan, J.D., Althoff, R.R, Whitlow, S., Cohen, NJ. (2000). Amnesia is a deficit in relational memory. *Psychological Science, 11,* 454-461.

Sato, N. & Nakamura, K. (2003). Visual response properties of neurons in the parahippocampal cortex of monkeys. *Journal of Neurophysiology, 90(2),* 876-886.

Saunders, R.C., Mishkin, M., & Aggleton, J.P. (2005). Projections from the entorhinal cortex, perirhinal cortex, presubiculum, and parasubiculum to the medial thalamus in macaque monkeys: identifying different pathways using disconnection techniques. *Experimental Brain Research, 167(1),* 1-16.

Schmolesky, M.T., Wang, Y., Hanes, D.P., Thompson, K.G., Leutgeb, S., Schall, J.D., Leventhal A.G. (1998). Signal timing across the macaque visual system. *Journal of Neurophysiology, 79(6),* 3272-8.

Seelke, A.M.H., Padberg, J.J., Disbrow, E., Purnell, S.M., Recanzone, G., Krubitzer, L. (2012). Topographic maps within Brodmann's area 5 of macaque monkeys. *Cerebral Cortex, 22(8),* 1834-1850.

Shen, K., Bezgin, G., Schirner, M., Ritter, P., Everling, S., McIntosh, A.R. (2018) A macaque connectome for large-scale network simulations in TheVirtualBrain. *bioRxiv* https://doi.org/10.1101/480905.

Shen, K., Bezgin, G., Selvam, R., McIntosh, A.R. & Ryan, J.D. (2016). An anatomical interface between memory and oculomotor systems. *Journal of Cognitive Neuroscience,* 28(11), 1772-1783.

Shen, K., Goulas, A., Grayson, D., Eusebio, J., Gati, J.S., Menon, R.S., McIntosh, A.R., Everling, S. (2019). Exploring the limits of network topology estimation using diffusion-based tractography and tracer studies in the macaque cortex. *NeuroImage, 191*, 81-92.

Shibutani, H., Sakata, H., Hyvarinen, J. (1984). Saccade and blinking evoked by microstimulation of the posterior parietal association cortex of the monkey. *Experimental Brain Research, 55(1),* 1-8.

Smith, C.N., Hopkins, R.O., Squire, L.R. (2006). Experience-dependent eye movements, awareness, and hippocampus-dependent memory. *Journal of Neuroscience, 26(44),* 11304-11312.

Smith, C.N. & Squire, L.R. (2017).When eye movements express memory for old and new scenes in the absence of awareness and independent of hippocampus. *Learning and Memory, 24(2),* 95-103.

Snyder, L.H., Grieve, K.L., Brotchie, P. & Andersen, R.A. (1998). Separate body- and world-reference representations of visual space in parietal cortex. *Nature, 394(6696),* 887-891.

Spiegler, A., Hansen, E.C., Bernard, C., McIntosh, A.R., Jirsa, V.K. (2016). Selective activation of resting-state networks following focal stimulation in a connectome-based network model of the human brain. *eNeuro, 3(5),* pii: ENEURO.0068-16.2016.

641 Sobotka, S., Nowicka, A., & Ringo, J. L. (1997). Activity linked to externally cued
642 saccades in single units recorded from hippocampal, parahippocampal, and
643 inferotemporal areas of macaques. Journal of Neurophysiology, 78, 2156–2163.
644 Suzuki, W. & Amaral, D.G. (1994). Topographic organization of the reciprocal
645 connections between the monkey entorhinal cortex and the perirhinal and
646 parahippocampal cortices. *Journal of Neuroscience, 14(3:2),* 1856-1877.
647 Tang, Q., Burgalossi, A., Ebbesen, C.L., Sanguinetti-Scheck, J.I., Schmidt, H., Tukker,
648 J.J., Naumann, R., Ray, S., Preston-Ferrer, P., Schmitz, D., Brecht, M. (2016).
649 Functional architecture of the rat parasubiculum. *Journal of Neuroscience, 36(7),*
650 2289-2301.
651 Voss, J.L., Bridge, D.J., Cohen, N.J., & Walker, J.A. (2017). A closer look at the
652 hippocampus and memory. *Trends in Cognitive Sciences, 21(8),* 577-588.
653 Warren, D.E., Duff, M.C., Tranel, D. & Cohen, N.J. (2010). Medial temporal lobe
654 damage impairs representation of simple stimuli. *Frontiers Human Neuroscience,*
655 *4,* 35.
656 Whitehead, J.C., Li, L., McQuiggan, D.A., Gambino, S.A., Binns, M.A. & Ryan, J.D.
657 (2018). Portable eyetracking-based assessment of memory decline. *Journal of*
658 *Clinical and Experimental Neuropsychology.* 2018 Mar 16:1-13. doi:
659 10.1080/13803395.2018.1444737. Electronic publication ahead of print.
660 Witter, M.P. and Amaral, D.G. 2004. Hippocampal formation. In *The rat nervous system*
661 (ed. G. Paxinos), pp. 635–704. Elsevier Academic Press, San Diego.
662 Witter, M.P., Doan, T.P., Jacobsen, B., Nilssen, E.S., Ohara, S. (2017). Architecture of
663 the entorhinal cortex: a review of entorhinal anatomy in rodents with some

comparative notes. *Frontiers in Systems Neuroscience,* https://doi.org/10.3389/fnsys.2017.00046

Vincent, J.L., Kahn, I., Van Essen, D.C., & Buckner, R.L. (2010). Functional connectivity of the macaque posterior parahippocampal cortex. *Journal of Neurophysiology, 103(2),* 793-800.

Vlachos, I., Aertsen, A., & Kumar, A. (2012). Beyond statistical significance: implications of network structure of neuronal activity. *PLoS Computational Biology,* Jan 8(1):e1002311. doi: 10.1371/journal.pcbi.1002311.

Yassa, M.A., Stark, C.E. (2011) Pattern separation in the hippocampus. *Trends in Neurosciences, 34*, 515–525.

Yeung, L-K., Olsen, R.K., Bild-Enkin, H., D'Angelo, M.C., Kacollja, A., McQuiggan, D., Keshabyan, A., Ryan, J.D. & Barense, M.D. (2017). Anterolateral entorhinal cortex volume predicted by altered intra-item configural processing. *Journal of Neuroscience, 37(22),* 5527-5538. Available online 4 May 2017. doi: 10.1523/JNEUROSCI.3664-16.2017.

Zeidman, P. & Maguire, E.A. (2016). Anterior hippocampus: the anatomy of perception, imagination, and episodic memory. *Nature Reviews Neuroscience, 17(3),* 173-182.

Zola, S.M., Squire, L.R., Teng, E., Stefanacci, L., Buffalo, E.A., & Clark, R.E. (2000). Impaired recognition memory in monkeys after damage limited to the hippocampal region. *Journal of Neuroscience, 20(1),* 451-463.

Table 1. Additional Generic 2D oscillator model parameters

Parameter	Value	Description
d	0.07674	Temporal scale factor
τ	1	Time-scale hierarchy parameter
f	1	Coefficient for fast variable cubic self-feedback term
e	0	Coefficient for fast variable quadratic self-feedback term
g	-0.1	Coefficient of fast variable linear self-feedback term
α	1	Coefficient for linear input term from slow to fast variable
γ	1	Additional scaling parameter for fast variable constant input I and long-range inputs
c	0	Coefficient for quadratic input term from fast variable to slow variable
b	-12.3038	Coefficient for linear input term from fast variable to slow variable
β	0	Coefficient for slow variable linear self-feedback term
a	0	Slow variable constant input term
I	0	Fast variable constant input term

Table 2. Activation times (ms) following stimulation of hippocampal subfields and medial temporal lobe regions. Only regions of interest (HC/MTL regions, oculomotor nodes, and regions that are involved in the shortest paths between HC/MTL and oculomotor nodes) are shown. S= subiculum, PrS = pre-subiculum, PaS=para-subiculum; ERC = entorhinal cortex; 35/36 = perirhinal cortex; TF/TH = parahippocampal cortex. *0* = stimulation onset; N/A = no response observed.

		Stimulated Node									
		CA3	**CA1**	**S**	**PrS**	**PaS**	**ERC**	**35**	**36**	**TF**	**TH**
Observation Node	**CA3**	*0*	48	31	37	27	0	21	20	48	1
	CA1	137	*0*	0	0	46	0	8	2	0	0
	S	115	17	*0*	26	37	0	16	10	0	0
	PrS	84	23	119	*0*	25	6	13	11	0	0
	PaS	350	17	96	28	*0*	50	15	0	0	32
	ERC	169	40	0	4	0	*0*	0	0	7	13
	35	567	6	21	49	50	0	*0*	0	9	19
	36	317	1	14	10	6	0	0	*0*	6	14
	TF	137	0	20	0	44	11	12	6	*0*	0
	TH	7	0	29	0	0	20	29	18	0	*0*
	7a	N/A	381	202	336	795	256	53	52	103	59
	V4	N/A	76	353	103	244	280	147	142	5	15
	V2	215	56	274	48	66	139	16	17	6	0
	Ig	N/A	11	63	75	189	11	4	6	21	13
	Pro	N/A	52	96	12	48	3	1	4	29	20
	5	N/A	322	50	92	555	249	129	141	69	64
	10	N/A	59	24	83	106	12	10	12	81	20
	11	N/A	12	68	74	166	10	7	8	38	48
	12	N/A	96	186	93	285	15	9	10	24	34
	13	N/A	10	18	62	132	8	7	11	19	19
	14	N/A	9	27	57	76	9	9	11	13	20
	23	N/A	165	384	12	231	43	37	52	24	13
	25	435	6	19	35	57	6	11	8	9	12
	32	N/A	38	63	88	89	10	13	14	14	17
	24	N/A	107	250	55	238	24	22	25	22	16
	46	N/A	84	135	15	187	12	9	11	17	23
	FEF	N/A	217	452	68	500	79	19	15	34	71

Table 3. Changes in activation times (ms) following a lesion of CA1 and stimulation of hippocampal subfields and medial temporal lobe regions. Values were determined by subtracting the intact stimulation times (Table 2) from lesioned activation times, such that slower responses are positive while faster responses are negative. S= subiculum, PrS = pre-subiculum, PaS=para-subiculum; ERC = entorhinal cortex; 35/36 = perirhinal cortex; TF/TH = parahippocampal cortex. *0* = stimulation onset; N/A = no response observed.

		Stimulated Node									
		CA3	**CA1**	**S**	**PrS**	**PaS**	**ERC**	**35**	**36**	**TF**	**TH**
Observation Node	**CA3**	*0*		-4	-2	0	0	0	0	-5	-1
	CA1										
	S	-10		*0*	-7	-4	0	-1	-1	0	0
	PrS	-4		-3	*0*	-1	-2	-1	-1	0	0
	PaS	-32		106	-7	*0*	-8	-1	0	0	-8
	ERC	-3		0	-1	0	*0*	0	0	-1	-1
	35	N/A		-1	0	0	0	*0*	0	-1	-3
	36	55		-2	-1	0	0	0	*0*	-1	-2
	TF	-19		214	0	-9	-3	-2	-1	*0*	0
	TH	0		327	0	0	-3	-4	-2	0	*0*
	7a	N/A		-2	1	-1	-2	-1	-1	-1	0
	V4	N/A		N/A	-4	-2	11	-2	-2	-1	-1
	V2	-3		N/A	-4	-1	-1	0	0	-1	0
	Ig	N/A		22	28	4	0	0	0	1	0
	Pro	N/A		3	0	1	1	0	0	0	0
	5	N/A		1	0	2	0	0	-1	0	0
	10	N/A		-1	-6	1	0	0	0	-7	-1
	11	N/A		25	11	3	0	0	0	1	-3
	12	N/A		10	-6	3	0	0	1	-2	-2
	13	N/A		1	17	2	0	0	0	0	-1
	14	N/A		0	17	1	0	0	0	0	-1
	23	N/A		N/A	0	0	0	0	0	0	0
	25	63		-2	14	2	0	0	0	0	-1
	32	N/A		0	-4	1	0	0	0	0	0
	24	N/A		33	-1	3	0	0	0	0	0
	46	N/A		1	0	2	0	0	0	-1	-1
	FEF	N/A		84	-3	5	0	0	0	-1	-1

Table 4. Changes in activation times (ms) following a lesion of PrS and stimulation of hippocampal subfields and medial temporal lobe regions. Values were determined by subtracting the intact stimulation times (Table 2) from lesioned activation times, such that slower responses are positive while faster responses are negative. S= subiculum, PrS = pre-subiculum, PaS=para-subiculum; ERC = entorhinal cortex; 35/36 = perirhinal cortex; TF/TH = parahippocampal cortex. *0* = stimulation onset; N/A = no response observed.

		Stimulated Node									
		CA3	**CA1**	**S**	**PrS**	**PaS**	**ERC**	**35**	**36**	**TF**	**TH**
Observation Node	**CA3**	*0*	-3	0		-1	0	0	0	-6	-1
	CA1	-17	*0*	0		-9	0	-1	-2	0	0
	S	-9	0	*0*		-3	0	-1	0	0	0
	PrS										
	PaS	-20	1	-3		*0*	-4	0	0	0	-8
	ERC	38	-3	0		0	*0*	0	0	-1	-3
	35	N/A	0	0		0	0	*0*	0	0	-3
	36	38	0	0		0	0	0	*0*	-1	-2
	TF	-14	0	1		-7	-2	-1	0	*0*	0
	TH	-1	0	-4		0	-4	-5	-2	0	*0*
	7a	N/A	-2	0		1	-2	-1	-1	-1	-1
	V4	N/A	-1	-3		-3	0	-2	-2	0	-1
	V2	-4	-1	-4		-2	-1	0	-1	-1	0
	Ig	N/A	0	1		2	0	0	0	1	0
	Pro	N/A	0	1		1	1	0	0	0	0
	5	N/A	3	1		12	5	0	-1	0	0
	10	N/A	-1	0		0	0	0	0	-5	-1
	11	N/A	0	0		2	0	0	0	-2	-5
	12	N/A	0	1		2	0	0	1	-1	-3
	13	N/A	0	0		1	0	0	0	-1	-1
	14	N/A	0	0		1	0	0	0	0	-1
	23	N/A	4	1		5	0	-1	0	0	0
	25	8	1	0		1	0	0	0	1	-1
	32	N/A	0	0		0	0	0	0	0	0
	24	N/A	1	3		3	1	0	0	0	-1
	46	N/A	-1	1		5	0	0	0	-1	-1
	FEF	N/A	0	4		18	0	0	0	0	-4

Table 5. Changes in activation times (ms) following a lesion of all hippocampal subfields and stimulation of medial temporal lobe regions. Values were determined by subtracting the intact stimulation times (Table 2) from lesioned activation times, such that slower responses are positive while faster responses are negative. S= subiculum, PrS = pre-subiculum, PaS=para-subiculum; ERC = entorhinal cortex; 35/36 = perirhinal cortex; TF/TH = parahippocampal cortex. *0* = stimulation onset; N/A = no response observed.

		Stimulated Node									
		CA3	**CA1**	**S**	**PrS**	**PaS**	**ERC**	**35**	**36**	**TF**	**TH**
Observation Node	**CA3**										
	CA1										
	S										
	PrS										
	PaS										
	ERC						*0*	0	0	-3	-4
	35						0	*0*	0	-1	-5
	36						0	0	*0*	-2	-3
	TF						-4	-3	-4	*0*	0
	TH						-6	-7	-4	0	*0*
	7a						0	-1	-1	-2	-1
	V4						14	-3	-3	-1	-1
	V2						-1	0	-1	-1	0
	Ig						0	0	0	1	0
	Pro						1	0	0	0	-1
	5						14	-1	-2	0	0
	10						0	0	0	-10	-2
	11						0	0	0	0	-7
	12						0	0	1	-3	-5
	13						0	0	0	-1	-2
	14						0	0	0	0	-2
	23						0	-1	0	0	-1
	25						0	0	0	0	-1
	32						0	0	0	-1	-1
	24						1	0	0	0	-1
	46						0	0	0	-1	-2
	FEF						0	0	0	-2	-5

Table 6. Changes in activation times (ms) following a lesion of the ERC and stimulation of hippocampal subfields and medial temporal lobe regions. Values were determined by subtracting the intact stimulation times (Table 2) from lesioned activation times, such that slower responses are positive while faster responses are negative. S= subiculum, PrS = pre-subiculum, PaS=para-subiculum; ERC = entorhinal cortex; 35/36 = perirhinal cortex; TF/TH = parahippocampal cortex. *0* = stimulation onset; N/A = no response observed.

		Stimulated Node									
		CA3	**CA1**	**S**	**PrS**	**PaS**	**ERC**	**35**	**36**	**TF**	**TH**
Observation Node	**CA3**	*0*	-8	127	-2	6		54	51	-6	-1
	CA1	-1	*0*	0	0	0		-1	-2	0	0
	S	-3	0	*0*	-2	2		-2	-1	0	0
	PrS	0	0	14	*0*	-1		-1	-1	0	0
	PaS	-3	0	0	0	*0*		-1	0	0	0
	ERC										
	35	-22	0	-1	4	34		*0*	0	-1	-3
	36	-17	-1	-2	-1	0		0	*0*	-1	-1
	TF	-1	0	1	0	-1		-1	0	*0*	0
	TH	0	0	0	0	0		-2	-1	0	*0*
	7a	N/A	-1	-2	0	22		-1	0	0	0
	V4	N/A	0	-3	0	0		0	0	0	0
	V2	0	0	-4	0	0		0	0	0	0
	Ig	N/A	0	2	2	28		0	-1	0	0
	Pro	N/A	0	98	0	1		-1	-1	0	0
	5	N/A	0	0	0	1		-2	-4	0	0
	10	N/A	-1	-1	4	75		-1	-1	-2	0
	11	N/A	0	15	2	139		-1	-1	-1	-2
	12	N/A	-1	107	-2	267		0	0	-1	-1
	13	N/A	0	1	3	108		0	-1	0	-1
	14	N/A	0	1	3	104		-1	-1	0	-1
	23	N/A	0	-5	0	1		-1	-1	0	0
	25	26	0	-3	0	45		-1	-1	0	-1
	32	N/A	0	70	20	86		-1	-1	0	0
	24	N/A	-1	96	-1	29		0	-1	0	-1
	46	N/A	-2	101	0	64		0	0	0	0
	FEF	N/A	-3	342	-2	106		-1	0	0	-1

Table 7. Changes in activation times (ms) following a combined lesion of areas TH and TF and stimulation of hippocampal subfields and medial temporal lobe regions. Values were determined by subtracting the intact stimulation times (Table 2) from lesioned activation times, such that slower responses are positive while faster responses are negative. S= subiculum, PrS = pre-subiculum, PaS=para-subiculum; ERC = entorhinal cortex; 35/36 = perirhinal cortex; TF/TH = parahippocampal cortex. *0* = stimulation onset; N/A = no response observed.

		Stimulated Node									
		CA3	**CA1**	**S**	**PrS**	**PaS**	**ERC**	**35**	**36**	**TF**	**TH**
Observation Node	**CA3**	*0*	115	-3	-1	-4	0	0	1		
	CA1	N/A	*0*	0	0	45	0	-1	-2		
	S	N/A	120	*0*	17	-5	0	-4	-2		
	PrS	N/A	185	-29	*0*	101	-6	-3	-2		
	PaS	N/A	23	16	33	*0*	-16	-4	0		
	ERC	N/A	-7	0	-3	0	*0*	0	0		
	35	N/A	0	0	-5	1	0	*0*	0		
	36	N/A	-1	-1	-1	0	0	0	*0*		
	TF										
	TH										
	7a	N/A	N/A	5	N/A	N/A	-4	-2	-2		
	V4	N/A	N/A	N/A	N/A	N/A	67	-7	0		
	V2	N/A	N/A	N/A	N/A	N/A	3	-1	-1		
	Ig	N/A	1	3	31	142	0	0	0		
	Pro	N/A	0	1	0	2	1	0	0		
	5	N/A	N/A	2	1	N/A	3	-1	-3		
	10	N/A	-4	-1	-4	10	0	0	0		
	11	N/A	0	0	-7	4	0	0	0		
	12	N/A	1	1	-5	35	0	0	1		
	13	N/A	0	1	-3	11	0	0	0		
	14	N/A	0	1	-5	3	0	0	0		
	23	N/A	N/A	N/A	0	N/A	-1	-1	0		
	25	N/A	0	0	-1	6	0	0	0		
	32	N/A	-1	0	11	6	0	0	0		
	24	N/A	46	21	3	412	1	1	0		
	46	N/A	7	1	-1	53	0	0	0		
	FEF	N/A	69	35	-5	N/A	1	0	0		

Table 8. Changes in activation times (ms) following a combined lesion of areas 35 and 36 and stimulation of hippocampal subfields and medial temporal lobe regions. Values were determined by subtracting the intact stimulation times (Table 2) from lesioned activation times, such that slower responses are positive while faster responses are negative. S= subiculum, PrS = pre-subiculum, PaS=para-subiculum; ERC = entorhinal cortex; 35/36 = perirhinal cortex; TF/TH = parahippocampal cortex. *0* = stimulation onset; N/A = no response observed.

		Stimulated Node									
		CA3	**CA1**	**S**	**PrS**	**PaS**	**ERC**	**35**	**36**	**TF**	**TH**
Observation Node	**CA3**	*0*	-5	-3	-1	-2	0			-3	0
	CA1	-2	*0*	0	0	-1	0			0	0
	S	-3	0	*0*	-1	-1	0			0	0
	PrS	0	0	-1	*0*	0	-2			0	0
	PaS	-22	1	-7	0	*0*	34			0	0
	ERC	-19	19	0	-3	0	*0*			-2	-2
	35										
	36										
	TF	-1	0	0	0	-1	-1			*0*	0
	TH	0	0	0	0	0	-2			0	*0*
	7a	N/A	15	-2	-1	17	93			0	0
	V4	N/A	1	2	1	2	19			0	0
	V2	1	0	-5	0	0	81			0	0
	Ig	N/A	0	-4	1	45	-1			0	-1
	Pro	N/A	7	8	0	2	0			1	0
	5	N/A	-1	0	-1	-5	18			0	0
	10	N/A	5	0	-3	22	-2			5	-1
	11	N/A	0	5	1	87	-2			1	-3
	12	N/A	17	26	-1	158	-3			-2	-2
	13	N/A	0	1	-1	23	-1			0	-1
	14	N/A	0	1	-3	13	-1			0	-1
	23	N/A	0	-3	0	-1	-2			0	0
	25	125	0	-1	-1	7	-1			1	-1
	32	N/A	1	3	-4	14	-1			0	0
	24	N/A	1	6	-1	6	-2			0	-1
	46	N/A	14	11	0	52	-1			-1	-1
	FEF	N/A	53	90	-2	83	-3			-2	0

Table 9. Changes in activation times (ms) following a combined lesion of areas V4, 7a, 5 and 23 and stimulation of hippocampal subfields and medial temporal lobe regions. Values were determined by subtracting the intact stimulation times (Table 2) from lesioned activation times, such that slower responses are positive while faster responses are negative. S= subiculum, PrS = pre-subiculum, PaS=para-subiculum; ERC = entorhinal cortex; 35/36 = perirhinal cortex; TF/TH = parahippocampal cortex. *0* = stimulation onset; N/A = no response observed.

		Stimulated Node									
		CA3	**CA1**	**S**	**PrS**	**PaS**	**ERC**	**35**	**36**	**TF**	**TH**
Observation Node	**CA3**	*0*	0	0	0	1	0	0	1	1	0
	CA1	-57	*0*	0	0	-6	1	-1	1	0	0
	S	-43	0	*0*	0	-2	0	-1	0	0	0
	PrS	-31	-1	-35	*0*	-2	-1	-3	-2	0	0
	PaS	-94	0	-4	0	*0*	-3	-1	0	0	0
	ERC	43	2	0	0	0	*0*	0	0	0	0
	35	N/A	1	2	2	8	0	*0*	0	1	0
	36	118	2	1	0	1	0	0	*0*	0	1
	TF	-54	0	1	0	-4	-1	-2	0	*0*	0
	TH	-2	0	-3	0	0	-4	-10	-4	0	*0*
	7a										
	V4										
	V2	-101	-11	-59	-7	-14	-68	-5	-6	-1	0
	Ig	N/A	0	-4	-2	11	1	1	0	0	-1
	Pro	N/A	2	8	1	8	1	-1	0	4	1
	5										
	10	N/A	0	0	-2	1	0	0	0	0	0
	11	N/A	0	1	0	10	0	0	0	3	-1
	12	N/A	5	12	-1	37	1	0	1	2	1
	13	N/A	1	1	-1	2	0	0	0	0	0
	14	N/A	1	0	-2	-2	0	0	0	0	0
	23										
	25	-57	1	1	0	3	0	0	0	1	0
	32	N/A	0	-2	-5	-4	0	0	0	0	0
	24	N/A	-12	-5	11	-24	-2	-1	-2	-2	-2
	46	N/A	8	24	1	48	1	1	1	2	1
	FEF	N/A	48	124	7	187	9	2	3	10	6